Special Issue Article

Advances in Mechanical Engineering

Advances in Mechanical Engineering
2015, Vol. 7(8) 1–8
© The Author(s) 2015
DOI: 10.1177/1687814015591735
aime.sagepub.com
SAGE

Axisymmetric stagnation-point flow of a third-grade fluid over a lubricated surface

M Sajid[1,2], M Ahmad[3], I Ahmad[3], M Taj[3] and A Abbasi[3]

Abstract

In this article, axisymmetric stagnation-point flow of a third-grade fluid over a disk lubricated with a power law fluid is considered. Due to thin lubrication layer of variable thickness, third-grade fluid experiences a partial slip on the surface. The flow problem is governed through a system of nonlinear partial differential equations with nonlinear boundary conditions. A nonsimilar solution is presented in this article by implementing hybrid homotopy analysis method. This method combines the features of homotopy analysis and shooting methods. The results varying from no-slip to full-slip case are discussed under the influence of pertinent parameters.

Keywords

Axisymmetric flow, third-grade fluid, lubricated surface, slip condition, hybrid homotopy analysis method

Date received: 2 January 2015; accepted: 15 May 2015

Academic Editor: Yunn-Lin Hwang

Introduction

The flows of non-Newtonian fluids have important role in several industrial and engineering processes. Newton's law of viscosity does not hold for such fluids, and their rheological properties cannot be explained by a single constitutive relationship. The relationship between shear stress and shear rate in the non-Newtonian fluids is nonlinear. The mathematical models based on the flows of non-Newtonian fluids are more nonlinear and have higher order derivative terms in the governing equations when compared with the Navier–Stokes equations. A glance at the literature shows that different constitutive relationships have been proposed for non-Newtonian fluids. Among these models, the differential-type fluids of second and third grades have got special attention of the researchers. Numerous studies are available for the flows of non-Newtonian fluids. Some recent studies may be directed in the investigations[1–8] and references therein.

The study of flow phenomenon over a lubricated surface has important applications in machinery components such as fluid bearings and mechanical seals. Coating is another major application including the preparation of thin films, printing, painting, and adhesives. In biological fluids, the applications of such flows include flow of red blood cells in narrow capillaries and of liquid flow in the lung and eye. A review of literature suggests that various attempts are available for the flow over a lubricated surface. Stagnation-point flow considered by Homann[9] in a rigid plate was discussed against a thin lubrication layer by Yeckel et al.[10] for the first time. An analytical study of flow of a viscous fluid flowing over another viscous fluid was

[1]Theoretical Physics Division, PINSTECH, Islamabad, Pakistan
[2]AS-ICTP, Trieste, Italy
[3]Department of Mathematics, University of Azad Jammu & Kashmir, Muzaffarabad, Pakistan

Corresponding author:
M Ahmad, Department of Mathematics, University of Azad Jammu & Kashmir, Muzaffarabad 13100, Pakistan.
Email: manzoorajku@gmail.com

Creative Commons CC-BY: This article is distributed under the terms of the Creative Commons Attribution 3.0 License (http://www.creativecommons.org/licenses/by/3.0/) which permits any use, reproduction and distribution of the work without further permission provided the original work is attributed as specified on the SAGE and Open Access pages (https://us.sagepub.com/en-us/nam/open-access-at-sage).

Downloaded from ade.sagepub.com by guest on December 7, 2015

carried out by Blyth and Pozrikidis.[11] A slip boundary condition was introduced by Andersson and Rousselet[12] for the flow over a lubricated rotating disk. Santra et al.[13] discussed the axisymmetric stagnation-point flow of a viscous fluid over a lubricated surface. In Santra et al.,[13] a similarity solution was obtained for the governing equations using numerical technique. Sajid et al.[14] extended the problem discussed by Santra et al.[13] by including a general slip boundary condition. Recently, in another article, Sajid et al.[15] analyzed the two-dimensional stagnation-point flow of a viscoelastic Walter-B fluid over a lubricated surface. They obtained a numerical solution using the hybrid method. The analysis of non-Newtonian fluid flows over a thin lubricated layer is an open area of research. This fact motivated us to discuss the axisymmetric stagnation-point flow of a third-grade fluid over a lubricated surface of variable thickness. Third-grade fluid is preferred in the sense that it can describe the shear thinning or thickening effects. The mathematical model for the axisymmetric stagnation-point flow of a third-grade fluid over a power law lubricant give rise to nonlinear differential equations with nonlinear boundary conditions. The hybrid homotopy analysis method (HAM)[16] is implemented to obtain the solution of this nonlinear problem. This method combines the features of HAM[17–23] and shooting method.[24] This article is organized as follows: section "Mathematical formulation" contains the details of the mathematical model considered in this article. The hybrid HAM is explained in detail in section "Hybrid homotopy analysis solutions." Section "Results and discussion" is devoted for the results and their discussion. The concluding remarks are included in section "Concluding remarks."

Mathematical formulation

Consider a steady, incompressible, axisymmetric stagnation-point flow of a third-grade fluid over a lubricated surface. The lubricant obeys the constitutive relationship of a power law fluid. Cylindrical coordinates (r, θ, z) are chosen to develop a mathematical model of the considered flow situation. The axisymmetric nature of flow suggests that all quantities are independent of θ, and azimuthal component of velocity vanishes identically. It is assumed that the power law lubricant spreads on the surface from a point source at origin and makes a thin layer of variable thickness $h(r)$. The constant flow rate of the lubricant is given by

$$Q = \int_0^{h(r)} U(r,z) 2\pi r dz \tag{1}$$

where $[U(r,z), 0, W(r,z)]$ is the velocity field for the lubricant. The equations that govern the axisymmetric flow of a third-grade fluid are

$$\frac{\partial u}{\partial r} + \frac{u}{r} + \frac{\partial w}{\partial z} = 0 \tag{2}$$

$$\rho\left(u\frac{\partial u}{\partial r} + w\frac{\partial u}{\partial z}\right) = -\frac{\partial P}{\partial r} + \frac{\partial \tau_{rr}}{\partial r} + \frac{\partial \tau_{rz}}{\partial z} + \frac{\tau_{rr} - \tau_{\theta\theta}}{r} \tag{3}$$

$$\rho\left(u\frac{\partial w}{\partial r} + w\frac{\partial w}{\partial z}\right) = -\frac{\partial P}{\partial z} + \frac{\partial \tau_{rz}}{\partial r} + \frac{\partial \tau_{zz}}{\partial z} + \frac{\tau_{rz}}{r} \tag{4}$$

where τ_{rr}, τ_{rz}, $\tau_{\theta\theta}$, and τ_{zz} are

$$\begin{aligned}\tau_{rr} &= 2\mu\frac{\partial u}{\partial r} + 2\alpha_1\\ &\left[u\frac{\partial^2 u}{\partial r^2} + w\frac{\partial^2 u}{\partial r\partial z} + \frac{\partial w}{\partial r}\left(\frac{\partial u}{\partial z} + \frac{\partial w}{\partial r}\right) + 2\left(\frac{\partial u}{\partial r}\right)^2\right]\\ &+ \alpha_2\left[\left(\frac{\partial u}{\partial z} + \frac{\partial w}{\partial r}\right)^2 + 4\left(\frac{\partial u}{\partial r}\right)^2\right]\\ &+ 4\beta_3\frac{\partial u}{\partial r}\left[\left(\frac{\partial u}{\partial z} + \frac{\partial w}{\partial r}\right)^2 + 2\left\{\left(\frac{\partial u}{\partial r}\right)^2 + \left(\frac{\partial w}{\partial z}\right)^2 + \left(\frac{u}{r}\right)^2\right\}\right]\end{aligned} \tag{5}$$

$$\begin{aligned}\tau_{rz} &= \mu\left(\frac{\partial u}{\partial z} + \frac{\partial w}{\partial r}\right) + 2\alpha_2\left(\frac{\partial u}{\partial z} + \frac{\partial w}{\partial r}\right)\left(\frac{\partial u}{\partial r} + \frac{\partial w}{\partial z}\right)\\ &\alpha_1\left[u\left(\frac{\partial^2 u}{\partial r\partial z} + \frac{\partial^2 w}{\partial r^2}\right) + w\left(\frac{\partial^2 u}{\partial z^2} + \frac{\partial^2 w}{\partial r\partial z}\right)\right.\\ &\left. + 3\left(\frac{\partial u}{\partial r}\frac{\partial u}{\partial z} + \frac{\partial w}{\partial r}\frac{\partial w}{\partial z}\right) + \frac{\partial u}{\partial z}\frac{\partial w}{\partial z} + \frac{\partial u}{\partial r}\frac{\partial w}{\partial r}\right] + 2\beta_3\left(\frac{\partial u}{\partial z} + \frac{\partial w}{\partial r}\right)\\ &\left[\left(\frac{\partial u}{\partial z} + \frac{\partial w}{\partial r}\right)^2 + 2\left\{\left(\frac{\partial u}{\partial r}\right)^2 + \left(\frac{\partial w}{\partial z}\right)^2 + \left(\frac{u}{r}\right)^2\right\}\right]\end{aligned} \tag{6}$$

$$\begin{aligned}\tau_{\theta\theta} &= 2\mu\frac{u}{r} + 2\alpha_1\left[\frac{u}{r}\frac{\partial u}{\partial r} + \frac{w}{r}\frac{\partial u}{\partial z} + \left(\frac{u}{r}\right)^2\right] + 4\alpha_2\left(\frac{u}{r}\right)^2\\ &+ 4\beta_3\frac{u}{r}\left[\left(\frac{\partial u}{\partial z} + \frac{\partial w}{\partial r}\right)^2 + 2\left\{\left(\frac{\partial u}{\partial r}\right)^2 + \left(\frac{\partial w}{\partial z}\right)^2 + \left(\frac{u}{r}\right)^2\right\}\right]\end{aligned} \tag{7}$$

$$\begin{aligned}\tau_{zz} &= 2\mu\frac{\partial w}{\partial z} + 2\alpha_1\\ &\left[u\frac{\partial^2 w}{\partial r\partial z} + w\frac{\partial^2 w}{\partial z^2} + \frac{\partial u}{\partial z}\left(\frac{\partial u}{\partial z} + \frac{\partial w}{\partial r}\right) + 2\left(\frac{\partial w}{\partial z}\right)^2\right]\\ &+ \alpha_2\left[\left(\frac{\partial u}{\partial z} + \frac{\partial w}{\partial r}\right)^2 + 4\left(\frac{\partial w}{\partial z}\right)^2\right]\\ &+ 4\beta_3\frac{\partial w}{\partial z}\left[\left(\frac{\partial u}{\partial z} + \frac{\partial w}{\partial r}\right)^2 + 2\left\{\left(\frac{\partial u}{\partial r}\right)^2 + \left(\frac{\partial w}{\partial z}\right)^2 + \left(\frac{u}{r}\right)^2\right\}\right]\end{aligned} \tag{8}$$

in which u and w are the radial and axial components of velocity in a third-grade fluid, respectively; μ is the viscosity; and α_1, α_2, and β_3 are the material parameters. The order and magnitude analysis results in the

Downloaded from ade.sagepub.com by guest on December 7, 2015

following equation that govern the boundary layer axisymmetric flow of a third-grade fluid

$$\rho\left(u\frac{\partial u}{\partial r}+w\frac{\partial u}{\partial z}\right)=-\frac{\partial P}{\partial r}+\mu\frac{\partial^2 u}{\partial z^2}+\alpha_1\left\{u\frac{\partial^3 u}{\partial r\partial z^2}+w\frac{\partial^3 u}{\partial z^3}+2\frac{\partial w}{\partial z}\frac{\partial^2 u}{\partial z^2}+\frac{\partial u}{\partial z}\frac{\partial^2 w}{\partial z^2}+3\frac{\partial u}{\partial r}\frac{\partial^2 u}{\partial z^2}\right\}-\alpha_2\left\{\frac{2u}{r}\frac{\partial^2 u}{\partial z^2}+\frac{1}{r}\left(\frac{\partial u}{\partial z}\right)^2\right\}+6\beta_3\left(\frac{\partial u}{\partial z}\right)^2\frac{\partial^2 u}{\partial z^2} \tag{9}$$

where ρ is the fluid density. The usual no-slip condition at the fluid–solid interface suggests that

$$U(r,\ 0)=0,\ W(r,\ 0)=0 \tag{10}$$

It is assumed that there is no variation in the velocity of the lubricant in the axial direction, therefore

$$W(r,\ z)=0,\quad \text{for } z\in[0,\ h(r)] \tag{11}$$

At the interface $z=h(r)$ where both the fluids interact, we impose the continuity of velocity and shear stress so that

$$u=U,\ w=W\quad \text{at } z=h(r) \tag{12}$$

$$\tau_{rz}=k\left(\frac{\partial U}{\partial z}\right)^n \tag{13}$$

where k is the consistency index and n is the power law index. Furthermore, equations (11) and (12) together yield

$$w(r,\ h(r))=0 \tag{14}$$

It is assumed that power law lubricant forms a very thin layer on the disk, and thus, following Joseph,[25] we impose boundary conditions (12)–(14) at the disk. The velocity at the free stream is assumed to be

$$u=cr,\ w=-2cz \tag{15}$$

where c is any positive constant. Following Santra et al.,[13] we assume that radial component U of the power law lubricant varies linearly in the following way

$$U(r,z)=\frac{\hat{U}(r)z}{h(r)} \tag{16}$$

where $\hat{U}(r)$ is the radial component of velocity for both the fluids at the interface. Hence, by substituting equation (16) into equation (1), one can obtain the thickness of the lubrication layer as follows

$$h(r)=\frac{Q}{\pi r\hat{U}(r)} \tag{17}$$

and hence the boundary condition given in equation (13) becomes

$$\tau_{rz}=k\left(\frac{\pi}{Q}\right)^n r^n u^{2n} \tag{18}$$

Introducing dimensionless variables

$$\eta=z\sqrt{\frac{c}{\nu}},\ u=crf'(\eta),\ w=-2\sqrt{c\nu}f(\eta) \tag{19}$$

The governing boundary value problem takes the form

$$f'''+2ff''-f'^2+1-2K_1\left(f''^2+ff^{iv}\right)-K_2\left(f''^2+2f'f'''\right)+3H\delta f''^2f'''=0 \tag{20}$$

$$f(0)=0,\ f''(0)\left[\begin{array}{c}1+2(K_1-K_2)f'(0)\\+H\left\{\delta f''^2(0)+12f'^2(0)\right\}\end{array}\right]-\lambda\left\{f'(0)\right\}^{2n}=0,\ f'(\infty)=1 \tag{21}$$

where

$$K_1=\frac{\alpha_1 c}{\mu},\ K_2=\frac{\alpha_2 c}{\mu},\ H=\frac{\beta_3 c^2}{\mu}\quad \text{and}\ \delta=\frac{cr^2}{\nu},\ \lambda=\frac{\sqrt{\frac{\nu}{c}}}{\frac{\mu}{k}\left(\frac{Qc}{\pi}\right)^{\frac{1}{3}}}=\frac{L_{visc}}{L_{lub}} \tag{22}$$

Here, we have expressed slip parameter λ as the ratio of viscous and lubrication length scales L_{visc} and L_{lub}, respectively. For small flow rates and highly viscous lubricants, L_{lub} is small, and hence, λ becomes large. For the case when $\lambda\to\infty$, the conventional no-slip condition $f'(0)=0$ is retrieved from equation (21). In the reverse case, slip coefficient λ vanishes, and one obtains the full-slip boundary condition. Hence, λ is an inverse measure of slip.

Hybrid homotopy analysis solutions

The boundary value problems (20) and (21) are first converted into two initial value problems using shooting method.[20] For this, we assume

$$f'(0)=s \tag{23}$$

and from equation (21), one obtains the value of $f''(0)$ and is given by

$$f''(0)=-\frac{2^{1/3}(1+2K_1s-2K_2s+12Hs^2)}{A}+\frac{A}{32^{1/3}H\delta} \tag{24}$$

where

Downloaded from ade.sagepub.com by guest on December 7, 2015

$$A = \left(27\delta^2 H^2 \lambda s^{2n} + \sqrt{729\delta^4 H^4 \lambda^2 s^{4n} + 108\delta^3 H^3 (1 + 2K_1 s - 2K_2 s + 12Hs^2)^3}\right)^{1/3}$$

Differentiating equations (20), (21), (23), and (24) with respect to s we obtain

$$\begin{aligned} &g''' + 2gf'' + 2fg'' - 2f'g' - 2K_1\left(2f''g'' + fg^{iv} + gf^{iv}\right) \\ &\quad - K_2(2f''g'' + 2f'g''' + 2g'f''') \\ &\quad + 3H\delta\left(2f''g''f''' + f''^2 g'''\right) = 0 \end{aligned} \tag{25}$$

$$\begin{aligned} &g(0) = 0,\ g'(0) = 1, \\ &g''(0) = -\frac{2^{1/3}(2K_1 - 2K_2 + 24Hs)}{A} \\ &\quad + \left(\frac{1}{32^{1/3}H\delta} - \frac{2^{1/3}(1 + 2K_1 s - 2K_2 s + 12Hs^2)}{A^2}\right)\frac{dA}{ds} \end{aligned} \tag{26}$$

It is pertinent to mention here that equations (20) and (25) have zero coefficient with the highest derivative term when $\eta = 0$ and $K_1 \to 0$; therefore, they cannot be integrated by a standard integration scheme. For numerical computations, we replaced ∞ by η_∞ and divided the domain $0 \le \eta \le \eta_\infty$ into subintervals $[(i-1)K, K]$, $i = 1, 2, 3, \ldots$, having fixed length H. The first-order initial value problems in each subinterval are

$$\begin{aligned} &\frac{df^i}{d\eta} = F^i,\ \frac{dF^i}{d\eta} = G^i,\ \frac{dG^i}{d\eta} = -2f^i G^i - 1 \\ &\quad + F^i 2 + 2K_1\left(G^i 2 + f^i\frac{d^2G^i}{d\eta^2}\right) \\ &\quad + K_2\left(G^i 2 + 2F^i\frac{dG^i}{d\eta}\right) - 3H\delta\left(G^i 2\frac{dG^i}{d\eta}\right) \end{aligned} \tag{27}$$

$$\begin{aligned} &\frac{dg^i}{d\eta} = Y^i,\ \frac{dY^i}{d\eta} = Z^i,\ \frac{dZ^i}{d\eta} = -2g^i G^i - 2f^i Z^i \\ &\quad + 2F^i Y^i + 2K_1\left(2G^i Z^i + f^i\frac{d^2Z^i}{d\eta^2} + g^i\frac{d^2G^i}{d\eta^2}\right) \\ &\quad + K_2\left(2G^i Z^i + 2F^i\frac{dZ^i}{d\eta} + 2Y^i\frac{dG^i}{d\eta}\right) \\ &\quad - 3H\delta\left(2G^i Z^i\frac{dG^i}{d\eta} + G^i 2\frac{dZ^i}{d\eta}\right) \end{aligned} \tag{28}$$

$$\begin{aligned} &f^1(0) = 0,\ F^1(0) = s, \\ &G^1(0) = -\frac{2^{1/3}(1 + 2K_1 s - 2K_2 s + 12Hs^2)}{A} \\ &\quad + \frac{A}{32^{1/3}H\delta},\ g^1(0) = 0,\ Y^1(0) = 1, \\ &Z^1(0) = -\frac{2^{1/3}(2K_1 - 2K_2 + 24Hs)}{A} \\ &\quad + \left(\frac{1}{32^{1/3}H\delta} - \frac{2^{1/3}(1 + 2K_1 s - 2K_2 s + 12Hs^2)}{A^2}\right)\frac{dA}{ds} \end{aligned} \tag{29}$$

Initial value problems (27)–(29) are solved using the HAM in each subinterval. The numerical values obtained through HAM at the end point of the ith subinterval are used as the initial conditions for the $(i+1)$th subinterval.

Zero-order deformation problems

The zero-order deformation problems are

$$(1-p)L\left[\bar{f}^i(\eta,p) - f_0^i(\eta)\right] = -p\left[\frac{d\bar{f}^i(\eta,p)}{d\eta} - \bar{F}^i(\eta,p)\right] \tag{30}$$

$$(1-p)L\left[\bar{F}^i(\eta,p) - F_0^i(\eta)\right] = -p\left[\frac{d\bar{F}^i(\eta,p)}{d\eta} - \bar{G}^i(\eta,p)\right] \tag{31}$$

$$\begin{aligned} &(1-p)L\left[\bar{G}^i(\eta,p) - G_0^i(\eta)\right] \\ &= -p\left[\frac{d\bar{G}^i(\eta,p)}{d\eta} + 2\bar{f}^i(\eta,p)\bar{G}^i(\eta,p) + 1 - \left(\bar{F}^i(\eta,p)\right)^2\right. \\ &-2K_1\left\{\left(\bar{G}^i(\eta,p)\right)^2 + \bar{f}^i(\eta,p)\frac{d^2\bar{G}^i(\eta,p)}{d\eta^2}\right\} \\ &- K_2\left\{\left(\bar{G}^i(\eta,p)\right)^2 + 2\bar{F}^i(\eta,p)\frac{d\bar{G}^i(\eta,p)}{d\eta}\right\} \\ &\left. + 3H\delta\left(\bar{G}^i(\eta,p)\right)^2\frac{d\bar{G}^i(\eta,p)}{d\eta}\right] \end{aligned} \tag{32}$$

$$(1-p)L\left[\bar{g}^i(\eta,p) - g_0^i(\eta)\right] = -p\left[\frac{d\bar{g}^i(\eta,p)}{d\eta} - \bar{Y}^i(\eta,p)\right] \tag{33}$$

$$(1-p)L\left[\bar{Y}^i(\eta,p) - Y_0^i(\eta)\right] = -p\left[\frac{d\bar{Y}^i(\eta,p)}{d\eta} - \bar{Z}^i(\eta,p)\right] \tag{34}$$

Downloaded from ade.sagepub.com by guest on December 7, 2015

$$(1-p)L\left[\bar{Z}^i(\eta,p)-Z_0^i(\eta)\right] = -p\left[\begin{array}{l}\dfrac{d\bar{Z}^i(\eta,p)}{d\eta}+2\bar{g}^i(\eta,p)\bar{G}^i(\eta,p)+2\bar{f}^i(\eta,p)\bar{Z}^i(\eta,p)-2\bar{F}^i(\eta,p)\bar{Y}^i(\eta,p)\\ -2K_1\left\{2\bar{G}^i(\eta,p)\bar{Z}^i(\eta,p)+\bar{g}^i(\eta,p)\dfrac{d^2\bar{G}^i(\eta,p)}{d\eta^2}+\bar{f}^i(\eta,p)\dfrac{d^2\bar{Z}^i(\eta,p)}{d\eta^2}\right\}\\ -K_2\left\{2\bar{G}^i(\eta,p)\bar{Z}^i(\eta,p)+2\bar{Y}^i(\eta,p)\dfrac{d\bar{G}^i(\eta,p)}{d\eta}+2\bar{F}^i(\eta,p)\dfrac{d\bar{Z}^i(\eta,p)}{d\eta}\right\}\\ +3H\delta\left\{2\bar{G}^i(\eta,p)\bar{Z}^i(\eta,p)\dfrac{d\bar{G}^i(\eta,p)}{d\eta}+\left(\bar{G}^i(\eta,p)\right)^2\dfrac{d\bar{Z}^i(\eta,p)}{d\eta}\right\}\end{array}\right] \tag{35}$$

where p and L are embedding parameter and auxiliary linear operator, respectively, and $f_0^i(\eta)$, $F_0^i(\eta)$, G_0^i, $g_0^i(\eta)$, $Y_0^i(\eta)$, and $Z_0^i(\eta)$ are chosen as initial guesses at each subinterval. Here, we take auxiliary parameter to be -1 and auxiliary function to be 1. This is due to the fact that convergence of the hybrid HAM is controlled through the subinterval length, that is, H, and the order of approximation.

*m*th-order deformation problems

The mth-order deformation problems in each subinterval are obtained by differentiating zero-order deformation problems m times with respect to p and are given by

$$L\left[f_m^i-\chi_m f_{m-1}^i\right] = -\frac{df_{m-1}^i}{d\eta}+F_{m-1}^i \tag{36}$$

$$L\left[F_m^i-\chi_m F_{m-1}^i\right] = -\frac{dF_{m-1}^i}{d\eta}+G_{m-1}^i \tag{37}$$

$$\begin{aligned}L\left[G_m^i-\chi_m G_{m-1}^i\right] &= -\frac{dG_{m-1}^i}{d\eta}+(\chi_m-1)\\ &+\sum_{k=0}^{m-1}\left[-2f_k^iG_{m-1-k}^i+F_k^iF_{m-1-k}^i\right.\\ &+2K_1\left\{G_k^iG_{m-1-k}^i+f_k^i\frac{d^2G_{m-1-k}^i}{d\eta^2}\right\}\\ &+K_2\left\{G_k^iG_{m-1-k}^i+2F_k^i\frac{dG_{m-1-k}^i}{d\eta}\right\}\\ &\left.-3H\delta\sum_{l=0}^{k}\left\{\frac{dG_{m-1-k}^i}{d\eta}G_{k-l}^iG_l^i\right\}\right]\end{aligned} \tag{38}$$

$$L\left[g_m^i-\chi_m g_{m-1}^i\right] = -\frac{dg_{m-1}^i}{d\eta}+Y_{m-1}^i \tag{39}$$

$$L\left[Y_m^i-\chi_m Y_{m-1}^i\right] = -\frac{dY_{m-1}^i}{d\eta}+Z_{m-1}^i \tag{40}$$

$$\begin{aligned}L\left[Z_m^i-\chi_m Z_{m-1}^i\right] &= -\frac{dZ_{m-1}^i}{d\eta}\\ &+\sum_{k=0}^{m-1}\left[2F_k^iY_{m-1-k}^i-2g_k^iG_{m-1-k}^i-2f_k^iZ_{m-1-k}^i\right.\\ &+2K_1\left\{2G_k^iZ_{m-1-k}^i+g_k^i\frac{d^2G_{m-1-k}^i}{d\eta^2}+f_k^i\frac{d^2Z_{m-1-k}^i}{d\eta^2}\right\}\\ &+2K_2\left\{G_k^iZ_{m-1-k}^i+Y_k^i\frac{dG_{m-1-k}^i}{d\eta}+F_k^i\frac{dZ_{m-1-k}^i}{d\eta}\right\}\\ &\left.-3H\delta\sum_{l=0}^{k}\left\{\frac{dZ_{m-1-k}^i}{d\eta}G_{k-l}^iG_l^i+2\frac{dG_{m-1-k}^i}{d\eta}G_{k-l}^iZ_l^i\right\}\right]\end{aligned} \tag{41}$$

$$\begin{aligned}&f_0^1(0)=0,\ F_0^1(0)=s,\\ &G_0^1(0) = -\frac{2^{1/3}(1+2K_1s-2K_2s+12Hs^2)}{A}\\ &+\frac{A}{32^{1/3}H\delta},\ g_0^1(0)=0,\ Y_0^1(0)=1,\\ &Z_0^1(0) = -\frac{2^{1/3}(2K_1-2K_2+24Hs)}{A}\\ &+\left(\frac{1}{32^{1/3}H\delta}-\frac{2^{1/3}(1+2K_1s-2K_2s+12Hs^2)}{A^2}\right)\frac{dA}{ds}\end{aligned} \tag{42}$$

$$\chi_m = \begin{cases}0, & m\le 1\\ 1, & m\ge 1\end{cases} \tag{43}$$

The final solutions in each subinterval are thus given by

$$[f,F,G,g,Y,Z]^i = \sum_{m=0}^{M}[f,F,G,g,Y,Z]_m^i \tag{44}$$

The solutions of the problems (36)–(43) proceed in the following manner. First s is assumed, and system of initial value problems is solved for $i=1$. From this solution, an initial condition for the second subinterval is evaluated, and a solution is obtained for this interval. This procedure is repeated, and an analytic solution is evaluated in each subinterval. A zero-finding algorithm

Downloaded from ade.sagepub.com by guest on December 7, 2015

Table 1. Comparisons of the numerical values of $f'(\eta)$ for the no-slip case ($\lambda \to \infty$) with Santra et al.[13] and White[26] for viscous fluid when $K_1 = K_2 = \delta = H = 0$.

η	Present $f''(0) = 1.31193769$ $f'(\eta)$	Santra et al.[13] $f''(0) = 1.31193769$ $f'(\eta)$	White[26] $f''(0) = 1.31194$ $f'(\eta)$
0.0	0.0	0.0	0.0
0.6	0.60870994	0.60870994	0.60871
1.2	0.89597727	0.89597727	0.89598
1.8	0.98315816	0.98315816	0.98316
2.4	0.99845935	0.99845935	0.99847
3.0	0.99992397	0.99992397	0.99993

Table 2. Numerical values of $f''(0)$ when $K_1 = 0.1$, $K_2 = 0.1$, $\delta = 1.0$, and $n = 1/3$.

λ	$H = 0.05$	$H = 0.10$	$H = 0.15$	$H = 0.20$	$H = 0.25$
0.1	0.062638	0.045925	0.036145	0.029765	0.025286
0.5	0.311059	0.238497	0.189931	0.156605	0.132762
1	0.585974	0.489095	0.403875	0.336385	0.285061
5	1.081374	1.048075	1.020699	0.998414	0.981302
10	1.119646	1.085586	1.058376	1.037805	1.025145
50	1.137523	1.102976	1.075842	1.056366	1.046788
100	1.138625	1.104048	1.076923	1.057528	1.048178

is chosen to evaluate the correct value of s which leads to $F_0^N(\eta_\infty) = 1$.

Results and discussion

The procedure explained in previous section is implemented in computational software mathematica for finding the numerical values at the end points of the subintervals and analytic solutions inside each subinterval. For the validity of the developed algorithm, a comparison of the present solutions with the existing results in the case of no slip when $\lambda \to \infty$ for the viscous fluid is given in Table 1. It is evident from the numerical values that our results agree well with the existing results. In Table 2, the numerical values of $f''(0)$ are given for different values of the slip and third-grade fluid parameters. These numerical values provide the missing conditions for obtaining the velocity profiles. Table 2 depicts that more drag force is required when one moves from full-slip to no-slip regime. In the case of full slip, almost zero drag force is experienced by the fluid at the surface, and therefore, slip has suppressed the effects of free stream velocity. The numerical values also show that drag force at the surface is a decreasing function of the third-grade fluid parameter. The influence of the pertinent parameters on the velocity profile is plotted in Figures 1–4.

Figure 1 is plotted to investigate the effects of slip parameter on the velocity field f'. The full-slip case is represented through the profile when $\lambda \to 0$, and the no-slip case is represented when $\lambda \to \infty$. It is clear from this figure that in the full-slip case, the slip on the surface dominates the effects of the free stream velocity, and almost no change is observed in the velocity throughout the semi-infinite domain. The momentum boundary layer thickness also decreases with increasing slip. The behavior of fluid parameter K_1 on the velocity profiles is presented in Figure 2. From this figure, we see that the velocity decreases by an increase in the parameter K_1. Figure 3 is displayed to analyze the

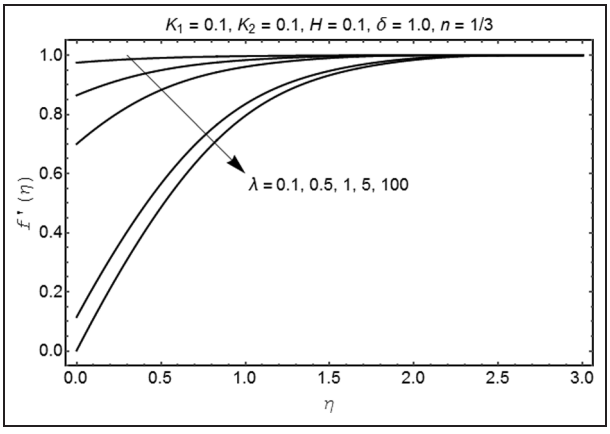

Figure 1. Influence of slip parameter λ on the fluid velocity $f'(\eta)$.

Downloaded from ade.sagepub.com by guest on December 7, 2015

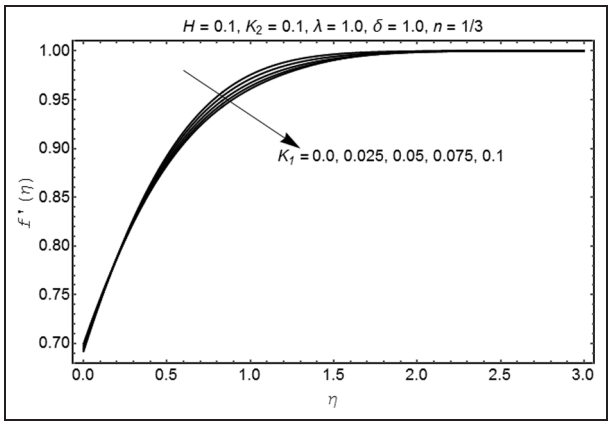

Figure 2. Influence of material parameter K_1 on the fluid velocity $f'(\eta)$.

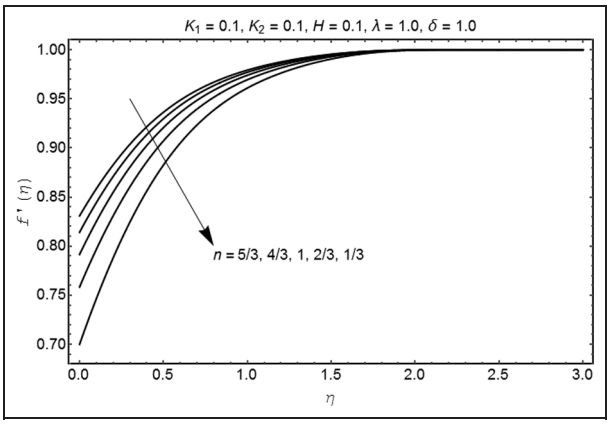

Figure 4. Influence of material parameter n on the fluid velocity $f'(\eta)$.

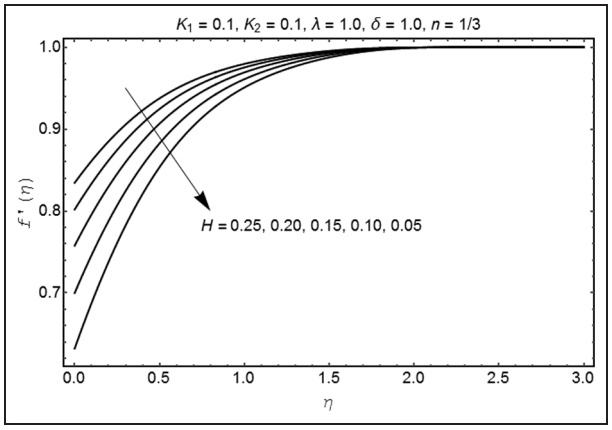

Figure 3. Influence of material parameter H on the fluid velocity $f'(\eta)$.

influence of third-grade fluid parameter on the velocity profile f'. This figure elucidate that the velocity increases, and the momentum boundary layer decreases by an increase in the third-grade fluid parameter. The effects of power law index n on the velocity profile f' are shown in Figure 4. The results show that for a shear thinning lubricant, the boundary layer thickness is more when compared to the shear thickening fluid. Furthermore, the velocity increases by an increase in the power law index. However, the boundary layer thickness is a decreasing function of the power law index.

Concluding remarks

The stagnation-point flow of a third-grade fluid over a disk lubricated with a power law fluid is discussed in this article. The governing equations are transformed to a nonsimilar ordinary differential equation subject to nonlinear boundary conditions. A hybrid HAM is employed for obtaining the quantities of interest. The findings of this study are as follows:

1. Slip increases the velocity and suppresses the boundary layer thickness;
2. Slip effects dominate the effects of free stream velocity;
3. Fluid velocity is an increasing function of third-grade fluid parameter;
4. Fluid velocity is more for a shear thickening lubricant when compared with a shear thinning lubricant;
5. Comparison of the obtained results with the existing literature is in an excellent agreement.

Declaration of conflicting interests

The author(s) declared no potential conflicts of interest with respect to the research, authorship, and/or publication of this article.

Funding

The author(s) disclosed receipt of the following financial support for the research, authorship, and/or publication of this article: This work was financially supported by Higher Education Commission (HEC) of Pakistan and AS-ICTP, Trieste, Italy.

References

1. Fetecau C, Mahmood A and Jamil M. Exact solutions for the flow of a viscoelastic fluid induced by a circular cylinder subject to a time dependent shear stress. *Commun Nonlinear Sci* 2010; 15: 3931–3938.
2. Sajid M and Hayat T. Non similar solution for the axisymmetric flow of a third grade fluid over a radially stretching sheet. *Acta Mech* 2007; 189: 193–205.
3. Ariel PD. Axisymmetric flow of a second grade fluid past a stretching sheet. *Int J Eng Sci* 2001; 39: 529–553.

Downloaded from ade.sagepub.com by guest on December 7, 2015

4. Rajagopal KR. A note on unsteady unidirectional flows of a non-Newtonian fluid. *Int J Nonlin Mech* 1982; 17: 369–373.
5. Hayat T, Wang Y, Siddiqui AM, et al. Couette flow of a third-grade fluid with variable magnetic field. *Math Mod Meth Appl S* 2004; 12: 1691–1706.
6. Shafique A, Nawaz M, Hayat T, et al. Magnetohydrodynamic axisymmetric flow of a third grade fluid between two porous disks. *Braz J Chem Eng* 2013; 30: 599–609.
7. Ahmad I. On unsteady boundary layer flow of a second grade fluid over a stretching sheet. *Add Theor Appl Mech* 2013; 6: 5–105.
8. Hayat T, Shafique A, Alsaedi A, et al. MHD axisymmetric flow of a third grade fluid between stretching sheets with heat transfer. *Comput Fluids* 2013; 86: 102–108.
9. Homann F. Der Einfluss grosser Zahigkeit bei der Stromung um den Zylinder und um die Kugel. *Z Angew Math Mech* 1936; 16: 153–164.
10. Yeckel A, Strong L and Middleman S. Viscous film flow in the stagnation region of the jet impinging on planar surface. *AIChE J* 1994; 40: 1611–1617.
11. Blyth MG and Pozrikidis C. Stagnation-point flow against a liquid film on a plane wall. *Acta Mech* 2005; 180: 203–219.
12. Andersson HI and Rousselet M. Slip flow over a lubricated rotating disk. *Int J Heat Fluid Fl* 2006; 27: 329–335.
13. Santra B, Dandapat BS and Andersson HI. Axisymmetric stagnation point flow over a lubricated surface. *Acta Mech* 2007; 194: 1–7.
14. Sajid M, Mahmood K and Abbas Z. Axisymmetric stagnation-point flow with a general slip boundary condition over a lubricated surface. *Chinese Phys Lett* 2012; 29: 1–4.
15. Sajid M, Javed T, Abbas Z, et al. Stagnation point flow of a viscoelastic fluid over a lubricated surface. *Int J Nonlin Sci Num* 2013; 14: 285–290.
16. Sajid M, Ahmad M and Ahmad I. Axisymmetric stagnation point flow of a second grade fluid over a lubricated surface. *Eur Int J Sci Tech*, in press.
17. Liao SJ. *The proposed homotopy analysis technique for the solution of non-linear problems*. PhD Thesis, Shanghai Jiao Tong University, Shanghai, China, 1992.
18. Liao SJ. *Beyond perturbation: introduction to the homotopy analysis method*. Boca Raton, FL: Chapman & Hall/CRC, 2003.
19. Liao SJ. *Homotopy analysis method in nonlinear differential equations*. Heidelberg: Springer & Higher Education Press, 2012.
20. Xu H and Pop I. Mixed convection flow of a nanofluid over a stretching surface with uniform free stream in the presence of both nanoparticles and gyrotactic microorganisms. *Int J Heat Mass Tran* 2014; 75: 610–623.
21. Xu H and Pop I. Fully developed mixed convection flow in a horizontal channel filled by a nanofluid containing both nanoparticles and gyrotactic microorganisms. *Eur J Mech B: Fluids* 2014; 46: 37–45.
22. Fan T and Xu H. New branches with algebraical behaviour for thermal boundary-layer flow over a permeable sheet. *Commun Nonlinear Sci* 2013; 18: 1162–1174.
23. Xu H and Pop I. Fully developed mixed convection flow in a vertical channel filled with a nanofluid. *Int Commun Heat Mass* 2012; 39: 1086–1092.
24. Na TY. *Computational methods in engineering boundary value problems*. New York: Academic Press, 1979.
25. Joseph DD. Boundary conditions for thin lubrication layers. *Phys Fluids* 1980; 23: 2356–2358.
26. White FM. *Viscous fluid flow*. 2nd ed. New York: McGraw-Hill, 1991, p.156.

Appendix 1

Notation

c	positive constant
f	dimensionless fluid velocity
F, G, Y, Z	derivatives of fluid velocities f, g
g	derivative of velocity with respect to s
h	thickness of the lubrication layer
i, m	indices
k	consistency index
K	interval length
K_1, K_2, H	dimensionless material parameters
L	auxiliary linear operator
L_{lub}	lubrication length scale
L_{visc}	viscous length scale
n	power law index
p	embedding parameter
P	fluid pressure
Q	volume flow rate of the lubricant
(r, θ, z)	cylindrical coordinates
s	missing condition
u, w	radial and axial velocity components of the third-grade fluid
U, W	radial and axial velocity components of the lubricant
$\hat{U}$	velocity for both the fluids at the interface
$\alpha_1, \alpha_2, \beta_3$	material parameters of the fluid
δ	local Reynolds number
η	dimensionless independent variable
η_∞	value of infinity for numerical calculations
λ	slip parameter
ρ	fluid density
$\tau_{rr}, \tau_{rz}, \tau_{\theta\theta}, \tau_{zz}$	stress components
χ_m	constant takes the value 0 or 1

Downloaded from ade.sagepub.com by guest on December 7, 2015